Temperature induced complex formation-deformation behavior of collagen model peptides and polyelectrolytes in aqueous solution

Ken Terao[a,*], Ryoko Kanenaga[a], Tasuku Yoshida[a], Kazunori Mizuno[b,1], Hans Peter Bächinger[b,c,*]

[a] *Department of Macromolecular Science, Osaka University, 1-1, Machikaneyama-cho, Toyonaka, Osaka, 560-0043, Japan*

[b] *Research Department, Shriners Hospital for Children, Portland, Oregon 97239, USA*

[c] *Department of Biochemistry and Molecular Biology, Oregon Health & Science University, Portland, Oregon 97239, USA*

* Corresponding authors. Tel.: +81 6 6850 5459; fax: +81 6 6850 5461.

E-mail addresses: kterao@chem.sci.osaka-u.ac.jp (K. Terao), hpb@shcc.org (H. P. Bächinger)

[1] Present Address. Nippi Research Institute of Biomatrix, 520-11 Kuwabara, Toride, Ibaraki 302-0017, Japan

ABSTRACT

Since the triple-helical collagen model peptides with a free *N*-terminus have three cationic groups at one end, it may have strong interactions with polyelectrolytes. In this study, complex formation behavior was investigated for sodium carboxymethyl amylose (NaCMA) + H-(Pro-Pro-Gly)$_{10}$-OH (PPG10), a collagen model peptide, in aqueous NaCl with ionic strength of 10 mM and 100 mM by means of small-angle X-ray scattering (SAXS) and circular dichroism at different temperatures. The previously reported [*Macromolecules* **2012**, *45*, 392-400] sodium polyacrylate (NaPAA) and H-(Gly-Pro-4-(*R*)-Hyp)$_9$-OH (GPO9) system was also investigated to elucidate complex formation nearby the transition temperature region between triple helix and single coil of the peptide. The complex formed near the melting temperature of the triple helices, confirmed that the triple helical structure is directly related to the complex formation.

1. Introduction

Intermolecular interaction between peptide and polyelectrolyte molecules is an important topic since ionic exchange is one of the most useful methods to purify or to analyze peptide molecules [1, 2]. Indeed, complex formation behaviors of proteins and polyelectrolytes are investigated by static scattering methods [3-5]. On the one hand, some collagen model peptides [6] (CMP or triple helical peptide, THP [7]) show fully thermo-reversible triple-helix – single chain conformational change in aqueous solution, and thus their detailed structure and thermodynamic properties are extensively studied to clarify the structure and the functionality of collagen *in vivo* [8-11]. Interestingly, three CMP molecules align in parallel and three *N*-termini locate nearby each other [10-12] even in aqueous solution [13, 14]. We recently found that the triple helical structure of CMP is stabilized in the presence of polyelectrolyte [15], and the complex consisting of H-(Gly-Pro-4-(*R*)-Hyp)$_9$-OH (GPO9) and sodium polyacrylic acid (NaPAA) of which chemical structures are shown in Fig. 1 are found in saline at low temperature [16]. The obtained particle scattering function data are well explained by the comb-like wormlike-chain model [17] as schematically shown in the graphical abstract and therefore we concluded that positively charged *N*-termini strongly interact attractively with anionic groups of NaPAA. This phenomenon is just observed for the one system and it is preferable to study other systems to confirm that this is due to the electrostatic interactions. Furthermore, it is still unclear if triple helix formation is directly related to complex formation since the complex formation-deformation behavior was just investigated at much higher (75 °C) and much lower (15 °C) temperatures than the conformational transition temperature (~45 °C) of GPO9.

We therefore made small-angle X-ray scattering and circular dichroism measurements for the sodium carboxymethyl amylose (NaCMA, Fig. 1) and H-(Pro-Pro-Gly)$_{10}$-OH (PPG10, Fig.

1) system in 100 mM and 10 mM aqueous NaCl at various temperatures. To investigate association-dissociation phenomena for the former system, SAXS measurements were also made for NaPAA and GPO9 solution at different temperatures including the transition region between triple helices and random coils.

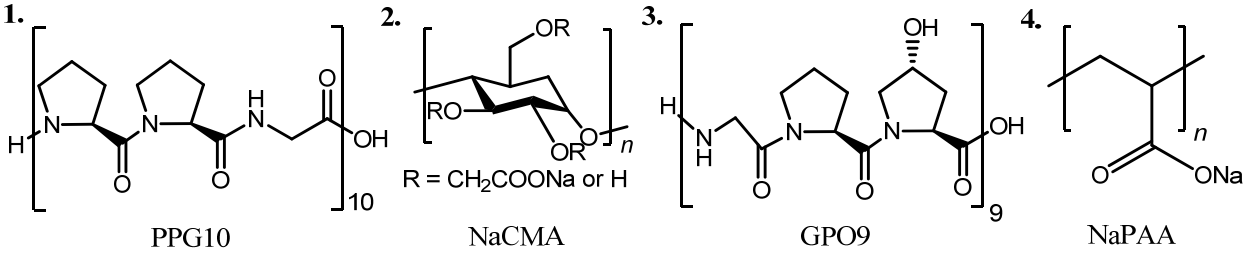

Fig. 1. Chemical structures of investigated samples. **1.** H-(Pro-Pro-Gly)$_{10}$-OH (PPG10), **2.** Sodium carboxymethyl amylose (NaCMA), **3.** H-(Gly-Pro-4-(*R*)-Hyp)$_9$-OH (GPO9), **4.** Sodium polyacrylic acid (NaPAA).

2. Experimental section

2.1. Samples and solvents

A previously investigated [16] sodium carboxymethyl amylose sample NaCMA26K prepared from enzymatically synthesized linear amylose [18, 19] and a sodium polyacrylate NaPAA267 were chosen as polyelectrolytes for this study. The weight-average molar mass M_w and the degree of substitution of NaCMA26K were determined to be 2.67×10^4 g mol^{-1} and 0.64, respectively, and M_w for the latter was reported as 2.51×10^4 g mol^{-1}. The previously investigated GPO9 sample and a PPG10 sample purchased from Peptide Institute Inc. were used for this study.

2.2. Measurements

Synchrotron-radiation small-angle X-ray scattering (SAXS) measurements for mixed solutions of NaCMA26K and PPG10 in 10 mM and 100 mM aqueous NaCl and those of NaPAA267 and GPO9 in 20 mM aqueous NaCl were performed at the BL-10C beamline in KEK-PF (Ibaraki, Japan) or at the BL40B2 beamline in SPring-8 (Hyogo, Japan) in the temperature range from 10 °C to 75 °C. The wavelength, camera length, and accumulation time were chosen to be 0.15 nm, 2000 mm, and 300 s in KEK-PF and 0.1 nm, 3000 mm, and 180 sec in SPring-8, respectively. The scattered light was detected by using R-AXIS VII imaging plate detectors (Rigaku, Japan). The beam center and the actual camera length were determined from the powder diffraction pattern of silver behenate and/or lead stearate. The circularly average method was utilized to obtain the scattering intensity $I(q)$ at each magnitude of the scattering vector q. Molar ratio of carboxylic unit of polyelectrolytes to the collagen model peptide α was chosen to be 3, 6, and 10 for NaCMA26K and PPG10 in 10 mM, $\alpha = 6$, 10, and 30 for NaCMA26K and PPG10 in 100 mM, and $\alpha = 10$ for NaPAA267 and GPO9 in 20 mM aqueous NaCl. For each system, the solvent and four solutions with different total mass concentration c of polyelectrolyte and peptide were filled in a quartz capillary cell with the diameter of 2.0 mm. The total concentration c range of the two solutes was set to be 1×10^{-3} – 1×10^{-2} g cm^{-3} for all systems. The optical constant K was determined from the excess scattering intensity $\Delta I(q)$ of NaCMA26K in saline solution or NaPAA267 + GPO9 at 15 °C assuming full complexation which was determined in our previous study [16] (see Results and Discussion).

If three components, that is, CMP, polyelectrolyte (NaCMA or NaPAA), and their complex exist in solution, the total excess scattering intensity $\Delta I(q)_{c=0}$ at infinite dilution can be expressed as

$$\left[\frac{\Delta I(q)}{Kc}\right]_{c=0} = w_1 \Delta z_1^2 M_1 P_1(q) + w_2 \Delta z_2^2 M_2 P_2(q) + w_3 \Delta z_3^2 M_3 P_3(q) \qquad (1)$$

Here, w_i, Δz_i, M_i, and $P_i(q)$ are the weight fraction in the total solute, the excess electron density, molar mass, and the particle scattering function of the component i, respectively. Now we assume components 1, 2, and 3 to be isolated (single coil or triple helical) PPG10 (or GPO9), molecularly dispersed NaCMA (or NaPAA), and their complex. The excess electron density Δz_i is related to the partial specific volume v_p [20]. The v_p value for NaCMA was determined to be 0.572 cm^3g^{-1} and 0.586 cm^3g^{-1} at 25 °C and 55 °C, respectively, for the solution dialyzed by 100 mM aqueous NaCl at 25 °C. In 10 mM aqueous NaCl, this value was found to be 0.591 cm^3g^{-1} and 0.612 cm^3g^{-1} at 25 °C and 55 °C, respectively. The v_p value for PPG10 was determined to be 0.711 cm^3g^{-1} and 0.746 cm^3g^{-1} in pure water at 15 °C and 75 °C, respectively. These values are used to calculate Δz_2 in saline at each temperature since PPG10 have up to two ionized groups in one peptide molecule, and therefore preferable adsorption effects may be negligible.

Circular dichroism measurements were performed for NaCMA26K and PPG10 in 10 mM NaCl, and NaPAA267 and GPO9 in 20 mM aqueous NaCl both at α = 10 with substantially the same concentration as the SAXS measurements by using JASCO J720WO spectropolarimeter with a Peltier thermostated cell holder and a rectangular cell with 1 mm path length. Temperature scans were recorded at a fixed wavelength and 6 °C h^{-1} to determine molar ellipticity $[\theta]$. Since the resultant $[\theta]$ obeyed straight lines both at high and low temperature ranges, those for triple helices ($[\theta]_{helix}$) and single coil ($[\theta]_{coil}$) were determined from the lines and then the helix content $F(T)$ at transition region was estimated from the equation as a function of temperature.

$$[\theta(T)] = F(T)[\theta(T)]_{\text{helix}} + [1 - F(T)][\theta(T)]_{\text{coil}} \quad (2)$$

3. Results and discussion

3.1. Scattering Intensity and Complex Formation at Low Temperature

Conventional Berry plots [21] for NaCMA26K + PPG10 in 10 mM aqueous NaCl are illustrated in Fig. 2(a) at three typical temperatures below and above the conformational transition temperature, that is, ~35 °C for PPG10, where subscript c = 0 means the value at infinite dilution. It should be noted that $[Kc/\Delta I(q)]^{1/2}$ data were irrespective of the total concentration c in the range of investigated c except for low-q region, indicating that complex behavior does not significantly depend on c, and hence the extrapolated values to infinite dilution reflect the molar mass of the complex in the concentration range investigated. While the Berry plots in 100 mM aqueous NaCl were substantially independent of temperature between 10 and 60 °C (not shown here), the $\Delta I(q)$ data in 10 mM aqueous NaCl significantly increase with lower temperatures, indicating complex formation at lower temperatures. It should be noted that the scattering intensity from dispersed peptide molecules is much smaller than that from NaCMA26K and its complex. Dashed lines indicate the initial slope to determine $\Delta I(0)$. The z-average radius of gyration $\langle S^2 \rangle_z$ was determined from the intercept and the slope of the lines. A similar temperature dependence was also found for NaPAA267 + GPO9 system as illustrated in Fig. 2(b).

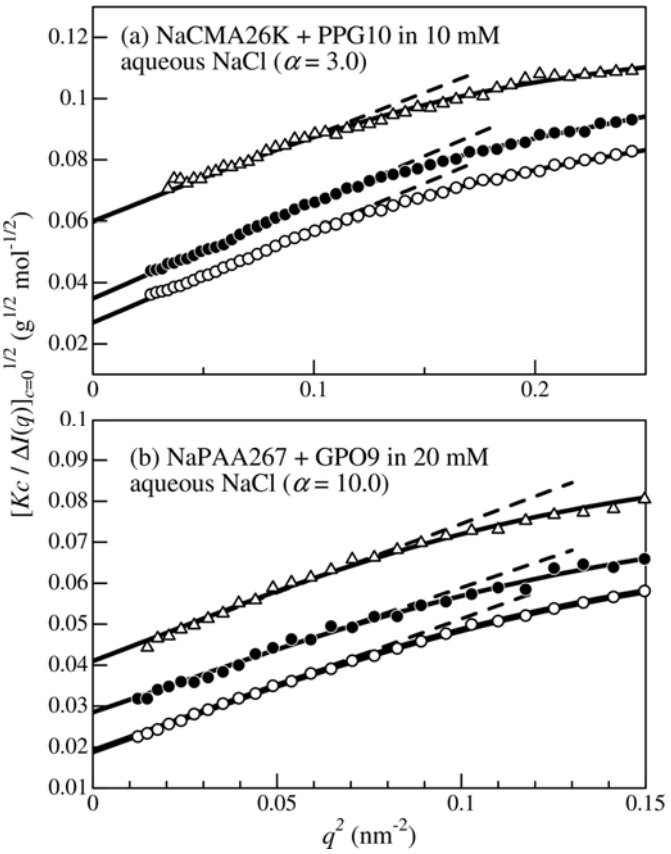

Fig. 2. Plots for $[Kc/\Delta I(q)]_{c=0}^{1/2}$ vs q^2 for (a) NaCMA26K + PPG10 ($\alpha = 3$) in 10 mM aqueous NaCl at 15 °C (unfilled circles), 40 °C (filled circles), 55 °C (triangles) and for (b) NaPAA267 + GPO9 in 20 mM aqueous NaCl ($\alpha = 10$) at 15 °C (unfilled circles), 60 °C (filled circles), 65 °C (triangles).

According to our previous paper [16], if some PPG10 chains form complex with NaCMA but higher order complexes do not exist in solution, the extrapolated value of $Kc/\Delta I(0)$ to $c = 0$ and $q = 0$ can be expressed as

$$\left(\frac{M_2}{n}+\frac{M_c}{\alpha}\right)\left[\frac{\Delta I(0)}{Kc}\right]_{c=0} = n\left(\Delta z_2 \frac{M_2}{n}+\Delta z_1 M_c f\right)^2 + m\Delta z_1{}^2 M_c{}^2\left(\frac{1}{\alpha}-f\right) \quad (3)$$

where M_2, M_c, n, and f denote the molar mass of NaCMA (or NaPAA), the molar mass of CMP, the number of carboxylic group of an NaCMA (or NaPAA) chain, and the degree of complexation of each NaCMA (or NaPAA) chain ($\leq \alpha^{-1}$). The f value becomes α^{-1} when all peptide molecules adsorb to NaCMA chains. The parameter m is unity for random coil CMP chain and 3 for triple helices. For no complexation ($f = 0$) and full complexation ($f = \alpha^{-1}$) limit, eq 3 reduces to

$$\left(\frac{M_2}{n}+\frac{M_c}{\alpha}\right)\left[\frac{\Delta I(0)}{Kc}\right]_{c=0}=\frac{\Delta z_2^2 M_2^2}{n}+\frac{m\Delta z_1^2 M_c^2}{\alpha}, \quad (f=0, \text{no complexation}) \tag{4}$$

$$\left(\frac{M_2}{n}+\frac{M_c}{\alpha}\right)\left[\frac{\Delta I(0)}{Kc}\right]_{c=0}=n\left(\Delta z_2\frac{M_2}{n}+\Delta z_1\frac{M_c}{\alpha}\right)^2, \quad \left(f=\frac{1}{\alpha}, \text{full complexation}\right) \tag{5}$$

Since the second term of the right hand side of eq 4 is much smaller than the first term for the present experimental condition, plots of $\sqrt{(M_2/n+M_c/\alpha)[\Delta I(0)/Kc]_{c=0}}$ against $1/\alpha$ becomes linear as illustrated in Fig. 3. In this figure, dot-dashed and dashed lines indicate calculated values from eq 4 with m = 1 and 3, respectively. Theoretical values from eq 5 for full complexation is shown as solid lines. Experimental data for NaCMA + PPG10 in 10 mM aqueous NaCl at 55 °C obey a straight line for no complexation (eq 4) at which all PPG10 chains behaves as random coil. Meanwhile, data points at 15 °C are much higher than that at 55 °C and the weight fraction αf of PPG10 forming complex with NaCMA was estimated to be 0.82, 0.80, and 0.72 for α = 10, 6, and 3, indicating that most of PPG10 chains form complex with NaCMA at high α but the degree of complexation f decreases with decreasing α. Similar results were also obtained for the NaPAA + GPO9 system [16] both in 20 mM and 100 mM aqueous NaCl.

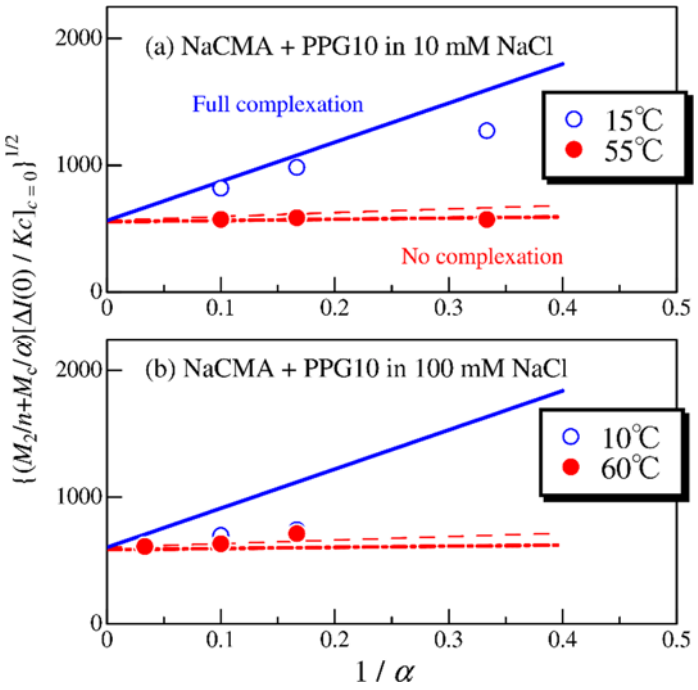

Fig. 3. Plots of $[(M_2/n + Mc/\alpha)\ (\Delta I(0)/Kc)_{c=0}]^{1/2}$ vs $1/\alpha$ for NaCMA + PPG10 in 10 mM (a) and 100 mM (b) aqueous NaCl at indicated temperatures. Solid, dashed, and dot-dashed lines indicate the calculated values by using eq 5 (full complexation), eq 4 (no complexation) with $m = 3$, and eq 4 with $m = 1$, respectively.

On the contrary, the experimental $\Delta I(0)$ for NaCMA + PPG10 in 100 mM at two temperatures below and above the conformational transition temperature of PPG10 locate nearby the lines from eq 4, indicating that intermolecular interactions between NaCMA and PPG10 significantly depend on ionic strength of the solvent since electrostatic attractive forces between PPG10 and NaCMA are screened by the added salt. This significant ionic strength dependence supports our previous conclusion that the complex formation is due to the electrostatic attraction force which was determined by using an uncharged peptide [16]. On the other hand, the complex formation behavior for the NaCMA + PPG10 system in 100 mM aqueous NaCl is significantly different than that for the NaPAA + GPO9 in the same solvent,

which shows full complex formation when α is not less than 10. This might be due to the difference of the linear charge density d_c of polyelectrolytes: d_c for NaCMA and NaPAA can be estimated to be 1.9 nm^{-1} and 3.8 nm^{-1}, respectively, from the chemical structure. It should be noted however that the complex formation behavior may also be caused by the chemical structure of peptide and polyelectrolytes.

3.2. Scattering function of the complex at low temperature

Fig. 4 indicates the Holtzer plots [22] for NaCMA with or without PPG10 in 10 mM NaCl at 15 °C. The particle scattering function $P_{thin}(q)$ for the thin linear wormlike chain is expressed as

$$P_{\text{thin}}(q) = \frac{2}{L^2}\int_0^L \lambda(L-t)\, I\left(\lambda^{-1}q;\lambda t\right) dt \tag{6}$$

where L and λ^{-1} denote the contour length and the Kuhn segment length (the stiffness parameter, twice of the persistence length), respectively. The former parameter L is related to the molar mass per unit contour length M_L by $L = M_w/M_L$. The characteristic function $I(\lambda^{-1}q; \lambda t)$ of the wormlike chain was calculated in terms of the approximate expression by Nakamura and Norisuye [17, 23]. The particle scattering function $P(q)$ for the touched-bead wormlike chain is expressed as [24, 25]

$$\begin{aligned} P(q) &= \left[F_{0b}(qd)\right]^2 P_{\text{thin}}(q) \\ F_{0b}(qd) &= 3\left(\frac{2}{qd}\right)^3\left(\sin\frac{qd}{2} - \frac{qd}{2}\cos\frac{qd}{2}\right) \end{aligned} \tag{7}$$

with d being the diameter of the bead. The data for NaCMA can be explained by this model with the appropriate parameters, that is M_L of 580 nm^{-1}g mol^{-1}, λ^{-1} of 5 nm, and d of 0.3 nm.

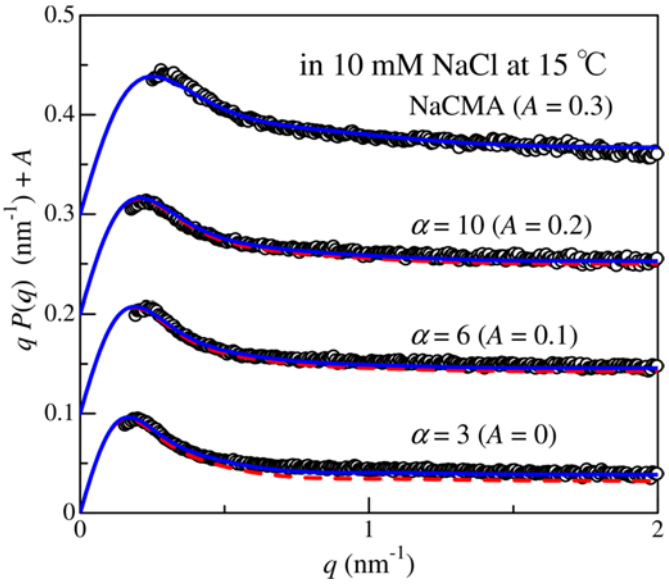

Fig. 4. Holtzer plots for NaCMA + PPG10 in 10 mM aqueous NaCl at 15 °C. Solid curves, calculated from eq 7 for NaCMA and from eq 11 for the mixtures. Dashed curves, calculated from eq 10 (not considering isolated PPG10 chains). The ordinate values are shifted by A.

If the obtained complex has a comb-like shape having N_S side chains consisting of triple helical (rodlike) PPG10 and their N-termini link to NaCMA by universal joints, the particle scattering function $P_{3,\mathrm{thin}}(q)$ for the complex without considering the chain thickness can be calculated as [16]

$$P_{3,\mathrm{thin}}(q) = \frac{2\left[\left(\Delta z_{\mathrm{m}} M_{\mathrm{L,m}}\right)^2 J_1 + \left(\Delta z_{\mathrm{s}} M_{\mathrm{L,s}}\right)^2 J_2 + \Delta z_{\mathrm{s}} \Delta z_{\mathrm{m}} M_{\mathrm{L,s}} M_{\mathrm{L,m}} J_3 + \left(\Delta z_{\mathrm{s}} M_{\mathrm{L,s}}\right)^2 J_4\right]}{\left(\Delta z_{\mathrm{m}} M_{\mathrm{m}} + N_{\mathrm{s}} \Delta z_{\mathrm{s}} M_{\mathrm{s}}\right)^2} \quad (8)$$

with

$$
\begin{aligned}
J_1 &= \int_0^{L_\mathrm{m}} \left(L_\mathrm{m} - t\right) I\left(\lambda^{-1} q; \lambda t\right) dt \\
J_2 &= \frac{N_\mathrm{s}\left[qL_\mathrm{s}\mathrm{Si}\left(qL_\mathrm{s}\right) + \cos\left(qL_\mathrm{s}\right) - 1\right]}{q^2} \\
J_3 &= \frac{\mathrm{Si}\left(qL_\mathrm{s}\right)}{q} \sum_{i=1}^{N_\mathrm{s}} \int_0^{L_\mathrm{m}} I\left(\lambda^{-1} q; \lambda \left|s_{i0} - s\right|\right) ds \\
J_4 &= \left[\frac{\mathrm{Si}\left(qL_\mathrm{s}\right)}{q}\right]^2 \sum_{i=1}^{N_\mathrm{s}-1} \sum_{j=i+1}^{N_\mathrm{s}} I\left[\lambda^{-1} q; \lambda\left(s_{j0} - s_{i0}\right)\right]
\end{aligned}
\tag{9}
$$

where subscripts m and s mean main and side chains and Si(x) being the sine integral. The original form of the equation is evaluated by Nakamura and Norisuye [17] for regular comb chains and by Huber and Burchard [26] for star polymers. From the obtained α and f, N_s is estimated to be 2.2, 3.6, and 6.4 for α = 10, 6, and 3, respectively. Since eq 8 is only applicable for integer N_s, $P_{3,\mathrm{thin}}(q)$ for the current N_s is estimated from interpolation method. Thus, $P_3(q)$ considering chain thickness by the touched bead model may be calculated from eq 7 when $P_{3,\mathrm{thin}}(q)$ is used instead of $P_\mathrm{thin}(q)$ as

$$
P_3\left(q\right) = \left[F_{0\mathrm{b}}\left(qd\right)\right]^2 P_{3,\mathrm{thin}}\left(q\right) \tag{10}
$$

If we choose $M_{\mathrm{L,s}}$ = 880 nm^{-1}g mol^{-1} from the length of the triple helical PPG10 (8.6 nm) [14], λ^{-1} of 6 nm, 7 nm, and 9 nm for α = 10, 6, and 3, and d = 0.3 nm, which is the same as that for NaCMA. The obtained λ^{-1} increases linearly with N_s and obeys a linear function of λ^{-1} / nm = 4.8 + 0.63 N_s. The calculated $P_3(q)$ drawn as dashed curves in Fig. 4 fairly reproduce the experimental data, but slightly underestimate the data at high q region. This is most likely due to the isolated triple helical peptide molecules. From eqs 1 and 3, the particle scattering function $P_\mathrm{mix}(q)$ for the mixture of the complex and collagen model peptide can be written as

$$P_{\mathrm{mix}}(q)=\frac{n\left(\Delta z_2 M_2 n^{-1}+\Delta z_1 M_{\mathrm{c}} f\right)^2 P_3(q)+m\Delta z_1{}^2 M_{\mathrm{c}}{}^2\left(\alpha^{-1}-f\right)P_1(q)}{n\left(\Delta z_2 M_2 n^{-1}+\Delta z_1 M_{\mathrm{c}} f\right)^2+m\Delta z_1{}^2 M_{\mathrm{c}}{}^2\left(\alpha^{-1}-f\right)} \tag{11}$$

where $m = 3$ and $P_1(q)$ can be calculated with the Bessel function $J_1(x)$ as

$$P_1(q)=\frac{2qL\,\mathrm{Si}(qL)+2\cos(qL)-2}{(qL)^2}\left[\frac{2J_1(qd/2)}{qd/2}\right]^2 \tag{12}$$

when all CMP molecules form triple helices. Assuming that the triple helical PPG10 has a length of 8.6 nm and a diameter of 1.5 nm, the calculated theoretical values drawn as solid curves nicely reproduce the experimental data, indicating that the wormlike comb model is suitable to describe complex formation of the NaCMA and PPG10 system as is the case with that for NaPAA + GPO9 [16]. The larger λ^{-1} for the main chain of this complex than that for NaCMA is likely due to the repulsive interaction between the main chain and PPG10. Indeed, the average radius of gyration from the scattering function at 15 °C was obtained to be 6.8 nm, 7.2 nm, and 8.2 nm for $\alpha = 10$, 6, and 3, respectively; these values are larger than 5.5 nm for NaCMA26K under the same conditions. It should be noted that these values can be explained by the same wormlike comb model (see eq 10 in ref [16]). Similar main chain elongation was also found for NaPAA + GPO9 system [16].

3.3. Temperature dependent complex formation

To elucidate the relationship between triple helix formation and complex formation, the scattering intensity for NaCMA + PPG10 in 10 mM aqueous NaCl ($\alpha = 10$) is plotted against temperature in Fig. 5. The data points at low temperatures are close to the solid lines for full

complexation ($f = \alpha^{-1}$) and the values decrease with raising temperature and approaches gradually to the value for molecularly disperse (dot-dashed line). Similar behavior was also found for the other α solutions in the same solvent and those for NaPAA + GPO9 in 20 mM aqueous NaCl. The f values were calculated for all data in terms of eq 3 to compare the resultant αf data with the helix content of CMPs (PPG10 or GPO9) obtained from circular dichroism measurements as shown in Fig. 6. The triple helical peptide chains dissociate with raising temperature nearby the melting temperature T_m of the triple helical peptides but it seems to be slightly higher than T_m both for all NaCMA + PPG10 systems (α = 10, 6, and 3) and the NaPAA + GPO9 system. These results suggest that single coil peptide chain may form a complex with polyelectrolytes only nearby T_m. According to our previous paper [13], the collagen model peptide having shorter chain length has a negative second virial coefficient at low temperature at which longer collagen model peptides including GPO9 form triple helix.

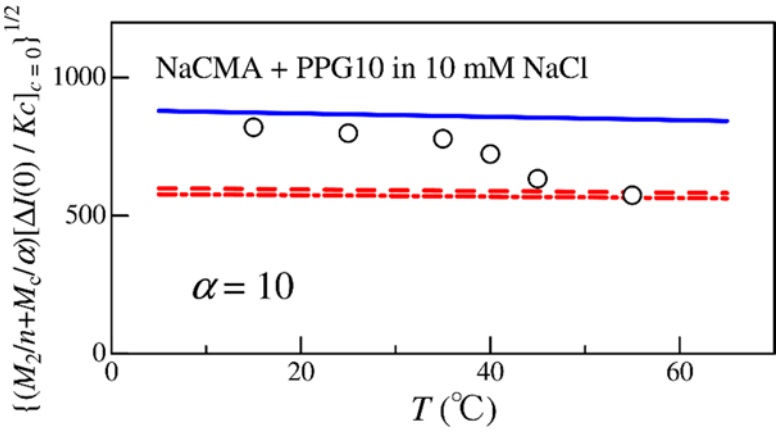

Fig. 5. Temperature dependence of $[(M_2/n + Mc/\alpha)\ (\Delta I(0)/Kc)_{c=0}]^{1/2}$ for NaCMA + PPG10 in 10 mM aqueous NaCl. Solid, dashed, and dot-dashed lines indicate the calculated values by using eq 5 (full complexation), eq 4 (no complexation) with m = 3, and eq 4 with m = 1, respectively.

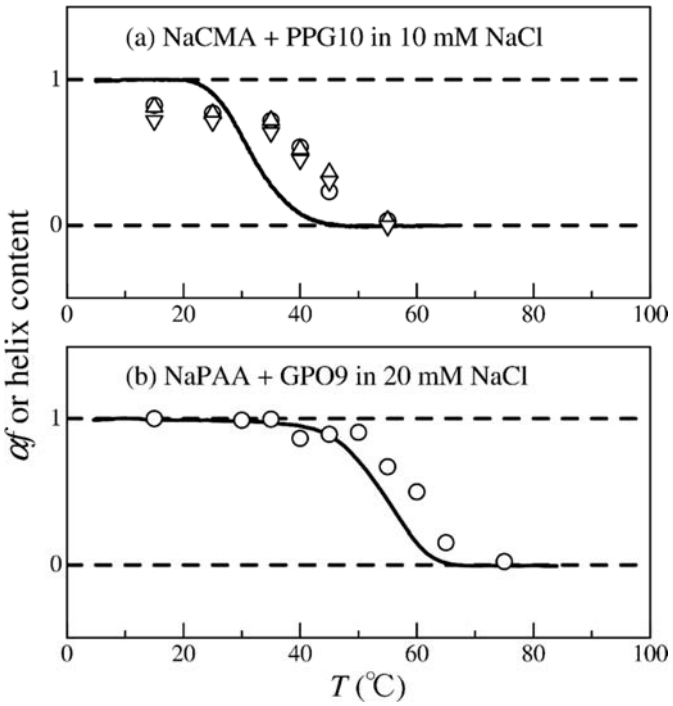

Fig. 6. Temperature dependence of αf (symbols) from SAXS measurements or helix contents from CD measurements (solid curves) for (a) NaCMA + PPG10 in 10 mM aqueous NaCl and for (b) NaPAA + GPO9 in 20 mM aqueous NaCl. Circles, triangles, and inverse triangles indicate $\alpha = 10$, $\alpha = 6$, and $\alpha = 3$, respectively.

One example of the temperature dependent scattering function for NaCMA + PPG10 ($\alpha = 6$) is shown in Fig. 7. Theoretical values can be calculated from eq 11 as is the case with the data in Fig. 4. It should be noted that we used $m = 3$ and rigid cylinder model for $P_1(q)$ at 15 °C and 25 °C as is the case for Fig. 4, but we chose $m = 1$ and the wormlike chain model with $\lambda^{-1} = 2$ nm and $M_L = 260$ nm^{-1}g mol^{-1} for the calculation of $P_1(q)$. These values are estimated from the random coil CMP chains [13]. If we estimate λ^{-1} from the above mentioned relationship (λ^{-1} / nm = 4.8 + 0.63 N_s) at each temperature, the theoretical values drawn as solid lines adequately explain the experimental data.

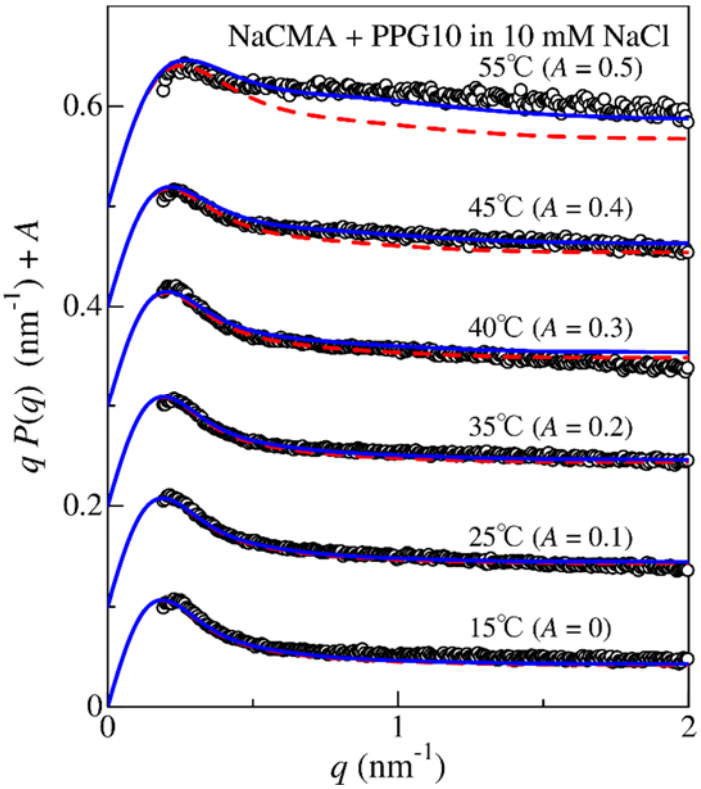

Fig. 7. Holtzer plots for NaCMA + PPG10 (α = 6) in 10 mM aqueous NaCl at indicated temperatures. Solid curves, calculated from eq 11 (see text). Dashed curves, calculated from eq 10 (not considering isolated PPG10 chains). The ordinate values are shifted by *A*.

The radius of gyration $\langle S^2 \rangle_{mix}$ for the mixture of the complex and collagen model peptide may be expressed by using the radius of gyration of the complex $\langle S^2 \rangle_3$ and isolated peptide $\langle S^2 \rangle_1$ as

$$\left\langle S^2 \right\rangle_{\mathrm{mix}} = \frac{n\left(\Delta z_2 M_2 n^{-1} + \Delta z_1 M_c f\right)^2 \left\langle S^2 \right\rangle_3 + m\Delta z_1{}^2 M_c{}^2 \left(\alpha^{-1} - f\right)\left\langle S^2 \right\rangle_1}{n\left(\Delta z_2 M_2 n^{-1} + \Delta z_1 M_c f\right)^2 + m\Delta z_1{}^2 M_c{}^2 \left(\alpha^{-1} - f\right)} \qquad (13)$$

where $\langle S^2 \rangle_3$ is related to the wormlike chain parameters by eq 10 in ref [16]. Considering the Kuhn length of NaPAA + GPO9 obeys a linear function of N_s [16] (λ^{-1} / nm = 2.8 + 0.54 N_s) as is the case with NaCMA + PPG10 system, $\langle S^2 \rangle_{mix}$ can be calculated with no fitting parameter. It should be noted that the contribution from the second term of eq 13 is negligibly small except for the data at the highest temperature. The obtained $\langle S^2 \rangle_{mix}$ values are substantially close to the experimental $\langle S^2 \rangle_z$ as shown in Fig. 8, indicating the current $\langle S^2 \rangle_z$ data can be explained by the above mentioned wormlike comb model.

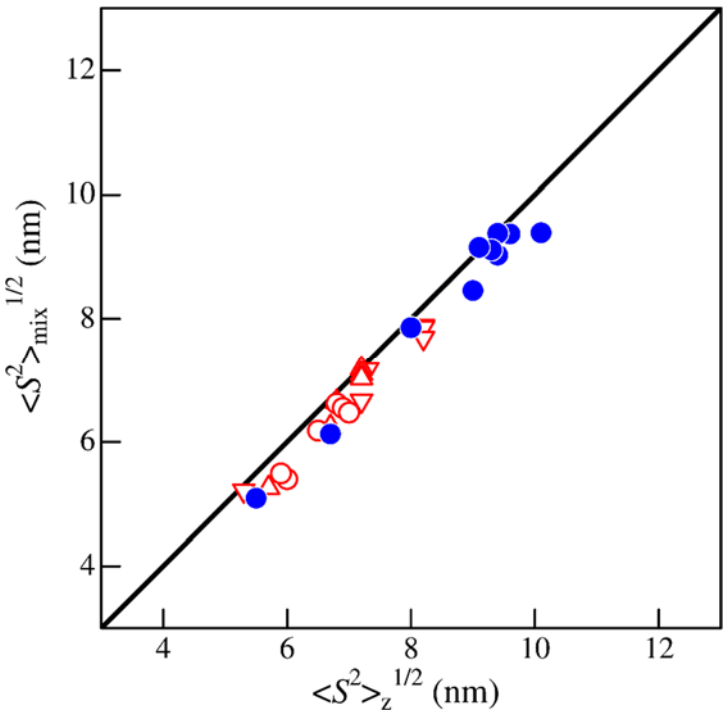

Fig. 8. Comparison between the experimental radius of gyration $\langle S^2 \rangle_z^{1/2}$ and the calculated values $\langle S^2 \rangle_{mix}$ from eq 13. Filled circles indicate the data for the NaPAA + GPO9 in 20 mM aqueous NaCl. Unfilled circles, triangles, and inverse triangles indicate $\alpha = 10$, $\alpha = 6$, and $\alpha = 3$, respectively, for NaCMA + PPG10 in 10 mM aqueous NaCl.

4. Conclusion

NaCMA forms a complex with the triple helical peptide PPG10 in 10 mM aqueous NaCl at low temperature and the obtained complex has a comb like structure of which the main chain is NaCMA and side chain is triple helical PPG10. However, NaCMA chains molecularly disperse in 100 mM solution even at low temperatures while NaPAA chains forms stable complex even in 100 mM aqueous NaCl. The complex dissociates with raising temperature near the melting point of triple helical peptide, indicating that the triple helical structure is definitely important to form the complex consisting of polyelectrolyte and CMP.

Acknowledgment

We are grateful to Professor Takahiro Sato in Osaka University for fruitful discussion and to Dr. Nobutaka Shimizu and Dr. Noriyuki Igarashi in KEK and Dr. Noboru Ohta in SPring-8 for SAXS measurements. The synchrotron radiation experiments were performed at the BL-10C in KEK-PF under the approval of the Photon Factory Program Advisory Committee (No. 2011G557) and at the BL40B2 in SPring-8 with the approval of the Japan Synchrotron Radiation Research Institute (JASRI) (Proposal No. 2013A1046). This work was partially supported by JSPS KAKENHI Grant Nos. 25410130 and 23350055.

References

1. Regnier FE. Science 1983;222:245-52.
2. Di Palma S, Hennrich ML, Heck AJ, Mohammed S. J Proteomics 2012;75:3791-813.
3. Tsuboi A, Izumi T, Hirata M, Xia JL, Dubin PL, Kokufuta E. Langmuir 1996;12:6295-303.
4. Gummel J, Cousin F, Boue F. Macromolecules 2008;41:2898-907.
5. Morfin I, Buhler E, Cousin F, Grillo I, Boue F. Biomacromolecules 2011;12:859-70.
6. Fallas JA, O'Leary LER, Hartgerink JD. Chem Soc Rev 2010;39:3510-27.

7. Fields GB. Organic & Biomolecular Chemistry 2010;8:1237-58.
8. Shoulders MD, Raines RT. Annu Rev Biochem 2009;78:929-58.
9. Berisio R, De Simone A, Ruggiero A, Improta R, Vitagliano L. J Pept Sci 2009;15:131-40.
10. Okuyama K. Connect Tissue Res 2008;49:299-310.
11. Okuyama K, Kawaguchi T. Kobunshi Ronbunshu 2010;67:229-47.
12. Okuyama K, Okuyama K, Arnott S, Takayanagi M, Kakudo M. J Mol Biol 1981;152:427-43.
13. Terao K, Mizuno K, Murashima M, Kita Y, Hongo C, Okuyama K, Norisuye T, Bächinger HP. Macromolecules 2008;41:7203-10.
14. Shikata T, Minakawa A, Okuyama K. J Phys Chem B 2009;113:14504-12.
15. Kita Y, Terao K, Sato T. Kobunshi Ronbunshu 2010;67:686-89.
16. Terao K, Kanenaga R, Sato T, Mizuno K, Bächinger HP. Macromolecules 2012;45:392-400.
17. Nakamura Y, Norisuye T. Brush-Like Polymers. In: Borsali R and Pecora R, editors. Soft Matter Characterization: Springer Netherlands, 2008. pp. 235-86.
18. Kitamura S, Yunokawa H, Mitsuie S, Kuge T. Polym J 1982;14:93-99.
19. Waldmann H, Gygax D, Bednarski MD, Randall Shangraw W, Whitesides GM. Carbohydr Res 1986;157:c4-c7.
20. Glatter O, Kratky O. Small Angle X-ray Scattering. London: Academic Press, 1982.
21. Berry GC. J Chem Phys 1966;44:4550-64.
22. Holtzer A. J Polym Sci 1955;17:432-34.
23. Nakamura Y, Norisuye T. J Polym Sci, Part B: Polym Phys 2004;42:1398-407.
24. Burchard W, Kajiwara K. Proc R Soc London, Ser A 1970;316:185-99.
25. Nagasaka K, Yoshizaki T, Shimada J, Yamakawa H. Macromolecules 1991;24:924-31.
26. Huber K, Burchard W. Macromolecules 1989;22:3332-36.